

Probing redshift-space distortions with phase correlations

Felipe O. Franco¹, Camille Bonvin¹, Danail Obreschkow^{2,3} and Kamran Ali^{2,3}

¹ *Département de Physique Théorique and Center for Astroparticle Physics (CAP),
University of Geneva, 24 quai Ernest Ansermet, CH-1211 Geneva, Switzerland*

² *International Centre for Radio Astronomy Research (ICRAR),
University of Western Australia, 35 Stirling Highway, Crawley WA 6009, Australia*

³ *ARC Centre of Excellence for All-sky Astrophysics (CAASTRO)*

(Dated: July 19, 2022)

Redshift-space distortions are a sensitive probe of the growth of large-scale structure. In the linear regime, redshift-space distortions are fully described by the multipoles of the two-point correlation function. In the non-linear regime, however, higher-order statistics are needed to capture the full information of the galaxy density field. In this paper, we show that the redshift-space line correlation function – which is a measure of Fourier phase correlations – is sensitive to the non-linear growth of the density and velocity fields. We expand the line correlation function in multipoles and we show that almost all of the information is encoded in the monopole, quadrupole and hexadecapole. We argue that these multipoles are highly complementary to the multipoles of the two-point correlation function, first because they are directly sensitive to the difference between the density and the velocity coupling kernels, which is a purely non-linear quantity; and second, because the multipoles are proportional to different combinations of f and σ_8 . Measured in conjunction with the two-point correlation function and the bispectrum, the multipoles of the line correlation function could therefore allow us to disentangle efficiently these two quantities and to test modified theories of gravity.

PACS numbers:

I. INTRODUCTION

Cosmological galaxy redshift surveys, like the 6dF Galaxy Redshift Survey [1], Sloan Digital Sky Survey [2], WiggleZ survey [3], VIPERS survey [4] or BOSS survey [5], map the distribution of galaxies in redshift-space. Since the redshift of galaxies is affected by their peculiar velocity, the observed galaxy distribution is slightly distorted with respect to the real-space galaxy distribution. In the linear regime, these redshift-space distortions modify the two-point correlation function and the power spectrum, by adding a quadrupole and an hexadecapole modulation in the signal [6, 7]. Measuring these multipoles has been one of the main goal of recent redshift galaxy surveys, see e.g. [8]. These measurements have been very successful and have provided constraints on modified theories of gravity [9]. Redshift-space distortions are indeed highly sensitive to the growth rate of perturbation f , which is generically modified in alternative theories of gravity.

In the non-linear regime, the multipoles of the correlation function are however not fully tracing the information present in galaxy surveys. The non-linear gravitational evolution of the density and peculiar velocity generates indeed a flow of information into higher-order statistics. An obvious choice to capture this flow of information is to look at the three-point correlation function (or Fourier-space bispectrum), see e.g. [10–12] and refs. therein. However this estimator is a three-dimensional function with significant redundancies with itself and the two-point statistics, making its computation and information analysis a complex task.

Various alternative observables have been constructed

in order to access information in the non-linear regime, see e.g. [13–16]. The goal of such observables is two-folds: first, part of the information present in the bispectrum has already been measured in the power spectrum. One can then wonder if it is possible to construct an observable which is less redundant with the power spectrum. And second, since the bispectrum is complicated in redshift-space, it would be interesting to construct an estimator which encodes the same type of information, but which is simpler to model.

In this paper, we study one possible alternative: the line correlation function. The line correlation function has been introduced in [17] and analytically modelled in real-space in [18]. This observable is constructed from correlations between the *phases* of the density field. Since the two-point function is only sensitive to the *amplitude* of the density field, it seems promising to use in conjunction an observable which is targeted to measure the phases (see [19–33] for other observables based on phase correlations). Fisher forecasts in real-space have shown that combining the line correlation function with the two-point correlation function does indeed improve parameter constraints on Λ CDM cosmology by up to a factor of 2 [34, 35]. The gain obtained from the line correlation function in the case of a Warm Dark Matter model or alternative theories of gravity, like the Symmetron and $f(R)$ model is even stronger [36].

Here we derive an expression for the line correlation function in redshift-space. We show that the line correlation function can be expanded in Legendre polynomials and that almost all of the information is encoded in the first even three multipoles, i.e. the monopole, quadrupole and hexadecapole, similarly to the two-point correlation

function. These multipoles are sensitive to the non-linear coupling kernels of the density and of the peculiar velocity. As such, the line correlation function provides a simple way to probe the non-linear evolution in redshift-space and consequently to constrain alternative theories of gravity in the non-linear regime, for example at the scales where screening mechanisms start to act. Note that our approach differs and complements the work of [37], which studies a modified version of the line correlation function (using an anisotropic window function) and is targeted to measure an anisotropic signal in two-dimensional Zel'dovich mock density fields.

The remainder of the paper is organised as follow. In Sec. II we derive an expression for the line correlation function in redshift-space, at second-order in perturbation theory. In Sec. III we expand the line correlation function in Legendre polynomials. We derive a general expression valid for any multipole n . In Sec. IV we calculate numerically the first multipoles in a Λ CDM universe and we show that the multipoles larger than $n = 4$ are negligible. We conclude in Sec. V.

II. THE LINE CORRELATION FUNCTION OF THE OBSERVED NUMBER COUNTS

Galaxy surveys measure the over-density of galaxies in redshift-space

$$\Delta(\mathbf{n}, z) = \frac{N(\mathbf{n}, z) - \bar{N}(z)}{\bar{N}(z)}, \quad (1)$$

where $N(\mathbf{n}, z)$ denotes the number of galaxies detected in a pixel situated at redshift z and in direction \mathbf{n} , and $\bar{N}(z)$ is the average number of galaxies per pixel at a given redshift. The Fourier transform of the galaxy over-density¹, $\Delta(\mathbf{k}, z)$, is characterised by an amplitude $|\Delta(\mathbf{k}, z)|$ and a phase

$$\epsilon_{\Delta}(\mathbf{k}, z) \equiv \frac{\Delta(\mathbf{k}, z)}{|\Delta(\mathbf{k}, z)|}. \quad (2)$$

The line correlation function of Δ is then defined as

$$\begin{aligned} \ell(\mathbf{r}, z) &= \frac{V^3}{(2\pi)^9} \left(\frac{r^3}{V}\right)^{3/2} \langle \epsilon_{\Delta}(\mathbf{s}, z) \epsilon_{\Delta}(\mathbf{s} + \mathbf{r}, z) \epsilon_{\Delta}(\mathbf{s} - \mathbf{r}, z) \rangle \\ &= \frac{V^3}{(2\pi)^9} \left(\frac{r^3}{V}\right)^{3/2} \int \int \int_{\substack{|\mathbf{k}_1|, |\mathbf{k}_2|, \\ |\mathbf{k}_3| \leq 2\pi/r}} d^3\mathbf{k}_1 d^3\mathbf{k}_2 d^3\mathbf{k}_3 e^{i(\mathbf{k}_1 + \mathbf{k}_2 + \mathbf{k}_3) \cdot \mathbf{s}} \\ &\quad \times e^{i(\mathbf{k}_2 - \mathbf{k}_3) \cdot \mathbf{r}} \langle \epsilon_{\Delta}(\mathbf{k}_1, z) \epsilon_{\Delta}(\mathbf{k}_2, z) \epsilon_{\Delta}(\mathbf{k}_3, z) \rangle, \end{aligned} \quad (3)$$

where $\epsilon_{\Delta}(\mathbf{s}, z)$ is the inverse Fourier transform of $\epsilon_{\Delta}(\mathbf{k}, z)$. As discussed in [17], the cutoff at high k has

¹ We use the Fourier convention $f(\mathbf{x}) = \int d^3\mathbf{k} e^{i\mathbf{x} \cdot \mathbf{k}} f(\mathbf{k})$ and $f(\mathbf{k}) = \int \frac{d^3\mathbf{x}}{(2\pi)^3} e^{-i\mathbf{x} \cdot \mathbf{k}} f(\mathbf{x})$.

been introduced to avoid the divergence of the line correlation function due to an infinite number of phase factors at arbitrarily small scales, which do not carry any information.

We start by calculating the three-point correlation function of the phase of $\Delta(\mathbf{k}, z)$. At linear order in perturbation theory, Δ is given by

$$\Delta(\mathbf{n}, z) = b \delta(\mathbf{n}, z) - \frac{1}{\mathcal{H}} \partial_r (\mathbf{v} \cdot \mathbf{n}), \quad (4)$$

where b is the linear bias, $\mathcal{H} = (da/d\eta)/a$ is the Hubble parameter in conformal time η , δ is the dark matter density field, \mathbf{v} is the peculiar velocity of galaxy and ∂_r denotes radial derivative. The second term in Eq. (4) represents the contribution from redshift-space distortions. We assume here for simplicity that the galaxy distribution is related to the dark matter distribution through a linear bias b . This assumption will break down at small scales and introduce a correction to the line correlation function, as shown in [34]. Note that Δ contains various other contributions, namely relativistic effects and lensing effects [38–40], but we neglect these terms here since we are mainly interested in small scales, where they are expected to be subdominant. We also neglect higher-order projection effects [41], that may be relevant in some intermediate regime.

In Fourier space, $\Delta(\mathbf{k}, z)$ takes the form

$$\Delta(\mathbf{k}, z) = b \delta(\mathbf{k}, z) - \frac{1}{\mathcal{H}} (\hat{\mathbf{k}} \cdot \mathbf{n})^2 V(\mathbf{k}, z), \quad (5)$$

where V is related to the Fourier transform of \mathbf{v} by

$$\mathbf{v}(\mathbf{k}, z) = -i \frac{\hat{\mathbf{k}}}{k} V(\mathbf{k}, z). \quad (6)$$

The three-point correlation function of the phase of $\Delta(\mathbf{k}, z)$, which enters in Eq. (3), can be expressed as

$$\langle \epsilon_{\Delta}(\mathbf{k}_1) \epsilon_{\Delta}(\mathbf{k}_2) \epsilon_{\Delta}(\mathbf{k}_3) \rangle = \int [d\theta] \mathcal{P}[\theta] \epsilon_{\Delta}(\mathbf{k}_1) \epsilon_{\Delta}(\mathbf{k}_2) \epsilon_{\Delta}(\mathbf{k}_3), \quad (7)$$

where $\mathcal{P}[\theta]$ is the probability distribution function of the field $\theta(\mathbf{k})$ defined through $\epsilon_{\Delta}(\mathbf{k}) = e^{i\theta(\mathbf{k})}$. Note that here we have dropped the dependence in redshift z in the argument of ϵ_{Δ} to ease the notation. Following [18, 30], we start by expressing the probability distribution function for $\Delta(\mathbf{k}, z)$ using the Edgeworth expansion [42–44], which is valid for mildly non-gaussian fields

$$\begin{aligned} \mathcal{P}[\Delta] &= N_G \exp \left(-\frac{1}{2} \int d^3\mathbf{k} \frac{\Delta(\mathbf{k}) \Delta(-\mathbf{k})}{P_{\Delta}(\mathbf{k})} \right) \left\{ 1 + \right. \\ &\quad \left. \frac{1}{3!} \int d^3\mathbf{p} d^3\mathbf{q} \frac{B_{\Delta}(\mathbf{p}, \mathbf{q}, -\mathbf{p} - \mathbf{q}) \Delta(-\mathbf{p}) \Delta(-\mathbf{q}) \Delta(\mathbf{p} + \mathbf{q})}{P_{\Delta}(\mathbf{p}) P_{\Delta}(\mathbf{q}) P_{\Delta}(\mathbf{p} + \mathbf{q})} \right\} \end{aligned} \quad (8)$$

where N_G is a normalisation factor. Here $P_{\Delta}(\mathbf{k})$ and $B_{\Delta}(\mathbf{p}, \mathbf{q}, \mathbf{k})$ are the power spectrum and bispectrum of Δ defined through

$$\langle \Delta(\mathbf{k}) \Delta(\mathbf{k}') \rangle = P_{\Delta}(\mathbf{k}) \delta_D(\mathbf{k} + \mathbf{k}'), \quad (9)$$

$$\langle \Delta(\mathbf{p}) \Delta(\mathbf{q}) \Delta(\mathbf{k}) \rangle = B_{\Delta}(\mathbf{p}, \mathbf{q}) \delta_D(\mathbf{p} + \mathbf{q} + \mathbf{k}). \quad (10)$$

Note that since redshift-space distortions break statistical isotropy, $P_\Delta(\mathbf{k})$ depends not only on the modulus of \mathbf{k} but also on its orientation with respect to the direction of observation \mathbf{n} . Similarly the bispectrum depends not only on the shape of the triangle but also on its orientation.

Following the derivation in [18], we first discretise the field $\Delta(\mathbf{k}) \rightarrow \Delta_{\mathbf{k}}$ for a finite survey volume and then we integrate over the amplitude $|\Delta_{\mathbf{k}}|$ to obtain the probability distribution function of the phase

$$\begin{aligned} \mathcal{P}(\{\theta_{\mathbf{k}}\}) \prod_{\mathbf{k} \in \text{uhs}} d\theta_{\mathbf{k}} = & \left\{ 1 + \frac{\sqrt{\pi}}{6} \sum_{\mathbf{p} \in \text{uhs}} b_\Delta(\mathbf{p}, \mathbf{p}) \cos(2\theta_{\mathbf{p}} - \theta_{2\mathbf{p}}) \right. \\ & + \frac{1}{3} \left(\frac{\sqrt{\pi}}{2} \right)^3 \sum_{\mathbf{p} \neq \mathbf{q} \in \text{uhs}} \left[b_\Delta(\mathbf{p}, \mathbf{q}) \cos(\theta_{\mathbf{p}} + \theta_{\mathbf{q}} - \theta_{\mathbf{p}+\mathbf{q}}) \right. \\ & \left. \left. + b_\Delta(\mathbf{p}, -\mathbf{q}) \cos(\theta_{\mathbf{p}} - \theta_{\mathbf{q}} + \theta_{\mathbf{p}-\mathbf{q}}) \right] \right\} \prod_{\mathbf{k} \in \text{uhs}} \frac{d\theta_{\mathbf{k}}}{2\pi}, \quad (11) \end{aligned}$$

where we have defined

$$b_\Delta(\mathbf{p}, \mathbf{q}) \equiv \sqrt{\frac{(2\pi)^3}{V}} \frac{B_\Delta(\mathbf{p}, \mathbf{q})}{\sqrt{P_\Delta(\mathbf{p})P_\Delta(\mathbf{q})P_\Delta(\mathbf{k})}}. \quad (12)$$

Inserting Eq. (11) into (7) we obtain in the continuous limit

$$\begin{aligned} \langle \epsilon_\Delta(\mathbf{k}_1) \epsilon_\Delta(\mathbf{k}_2) \epsilon_\Delta(\mathbf{k}_3) \rangle = & \quad (13) \\ & \frac{(2\pi)^3}{V} \left(\frac{\sqrt{\pi}}{2} \right)^3 b_\Delta(\mathbf{k}_1, \mathbf{k}_2, \mathbf{k}_3) \delta_D(\mathbf{k}_1 + \mathbf{k}_2 + \mathbf{k}_3). \end{aligned}$$

To calculate (13) explicitly we need an expression for $b_\Delta(\mathbf{k}_1, \mathbf{k}_2, \mathbf{k}_3)$. We work at second order in perturbation theory, where the density field $\delta^{(2)}$ and the velocity field $V^{(2)}$ take the form

$$\begin{aligned} \delta^{(2)}(\mathbf{k}, z) = & \int d^3\mathbf{q}_1 \int d^3\mathbf{q}_2 \delta_D(\mathbf{k} - \mathbf{q}_1 - \mathbf{q}_2) \\ & F_2(\mathbf{q}_1, \mathbf{q}_2) \delta^{(1)}(\mathbf{q}_1, z) \delta^{(1)}(\mathbf{q}_2, z), \quad (14) \end{aligned}$$

$$\begin{aligned} V^{(2)}(\mathbf{k}, z) = & -\mathcal{H}(z) f(z) \int d^3\mathbf{q}_1 \int d^3\mathbf{q}_2 \delta_D(\mathbf{k} - \mathbf{q}_1 - \mathbf{q}_2) \\ & G_2(\mathbf{q}_1, \mathbf{q}_2) \delta^{(1)}(\mathbf{q}_1, z) \delta^{(1)}(\mathbf{q}_2, z). \quad (15) \end{aligned}$$

Here $\delta^{(1)}$ denotes the linear density field,

$$f = \frac{d \ln D_1}{d \ln a} \quad (16)$$

is the growth rate (D_1 being the growth function) and the non-linear kernels are given by [45, 46]

$$\begin{aligned} F_2(\mathbf{k}_1, \mathbf{k}_2) = & \frac{1 + \epsilon_F}{2} + \frac{\hat{\mathbf{k}}_1 \cdot \hat{\mathbf{k}}_2}{2} \left(\frac{k_1}{k_2} + \frac{k_2}{k_1} \right) \\ & + \frac{1 - \epsilon_F}{2} \left(\hat{\mathbf{k}}_1 \cdot \hat{\mathbf{k}}_2 \right)^2, \quad (17) \end{aligned}$$

$$\begin{aligned} G_2(\mathbf{k}_1, \mathbf{k}_2) = & \epsilon_G + \frac{\hat{\mathbf{k}}_1 \cdot \hat{\mathbf{k}}_2}{2} \left(\frac{k_1}{k_2} + \frac{k_2}{k_1} \right) \\ & + (1 - \epsilon_G) \left(\hat{\mathbf{k}}_1 \cdot \hat{\mathbf{k}}_2 \right)^2, \quad (18) \end{aligned}$$

with $\epsilon_F \simeq (3/7) \Omega_m(z)^{-1/143}$ and $\epsilon_G = \epsilon_F + (3/2)(\epsilon_F - 3/7)$. The kernels depend therefore very mildly on z through ϵ_F and ϵ_G .

Inserting this into (5) we obtain for Δ at second order

$$\begin{aligned} \Delta^{(2)}(\mathbf{k}, z) = & \int d^3\mathbf{q}_1 \int d^3\mathbf{q}_2 \delta_D(\mathbf{k} - \mathbf{q}_1 - \mathbf{q}_2) \\ & \left[bF_2(\mathbf{q}_1, \mathbf{q}_2) + f(\hat{\mathbf{k}} \cdot \mathbf{n})^2 G_2(\mathbf{q}_1, \mathbf{q}_2) \right] \\ & \times \delta^{(1)}(\mathbf{q}_1, z) \delta^{(1)}(\mathbf{q}_2, z). \quad (19) \end{aligned}$$

Combining this with the first order expression for Δ

$$\Delta^{(1)}(\mathbf{k}, z) = \left[b + f(\hat{\mathbf{k}} \cdot \mathbf{n})^2 \right] \delta^{(1)}(\mathbf{k}, z), \quad (20)$$

we obtain

$$\begin{aligned} b_\Delta(\mathbf{k}_1, \mathbf{k}_2, \mathbf{k}_3) = & 2 \sqrt{\frac{(2\pi)^3}{V}} \\ & \times \left[W_2(\mathbf{k}_1, \mathbf{k}_2, \mathbf{k}_3, \mathbf{n}) \sqrt{\frac{P_L(k_1, z) P_L(k_2, z)}{P_L(k_3, z)}} + \text{cyc} \right], \quad (21) \end{aligned}$$

where P_L denotes the linear power spectrum of δ at redshift z and

$$W_2(\mathbf{k}_1, \mathbf{k}_2, \mathbf{k}_3, \mathbf{n}) \equiv \frac{bF_2(\mathbf{k}_1, \mathbf{k}_2) + (\hat{\mathbf{k}}_3 \cdot \mathbf{n})^2 f G_2(\mathbf{k}_1, \mathbf{k}_2)}{b + (\hat{\mathbf{k}}_3 \cdot \mathbf{n})^2 f}. \quad (22)$$

We see that the phase correlation of the observed number count Δ is sensitive to the non-linear coupling kernel of the density field F_2 , to the non-linear coupling kernel of the velocity field G_2 , and to the growth rate f . Since redshift-space distortions are not isotropic, the phase correlations depend on the direction of observation \mathbf{n} . Note that here we work in the distant-observer approximation, where \mathbf{n} is the same for all galaxies.

The line correlation function is obtained by inserting (21) and (13) into (3). We get

$$\begin{aligned} \ell(\mathbf{r}, z) = & \frac{r^{9/2}}{8\sqrt{2}(2\pi)^3} \iint_{\substack{|\mathbf{k}_1|, |\mathbf{k}_2|, \\ |\mathbf{k}_1 + \mathbf{k}_2| \leq 2\pi/r}} d^3\mathbf{k}_1 d^3\mathbf{k}_2 \\ & W_2(-\mathbf{k}_1 - \mathbf{k}_2, \mathbf{k}_1, \mathbf{k}_2, \mathbf{n}) \sqrt{\frac{P_L(|\mathbf{k}_1 + \mathbf{k}_2|, z) P_L(k_1, z)}{P_L(k_2, z)}} \\ & \left[e^{i(\mathbf{k}_1 - \mathbf{k}_2) \cdot \mathbf{r}} + e^{i(\mathbf{k}_1 + 2\mathbf{k}_2) \cdot \mathbf{r}} + e^{-i(2\mathbf{k}_1 + \mathbf{k}_2) \cdot \mathbf{r}} \right]. \quad (23) \end{aligned}$$

Here we have used the Dirac Delta function to rewrite the three permutations in (21) with the same kernel W_2 multiplied by three different exponentials. In this way, the kernel W_2 depends on the direction of observation \mathbf{n} only through its scalar product with \mathbf{k}_2 . We will see that this property is useful to solve analytically some of the integrals in (23).

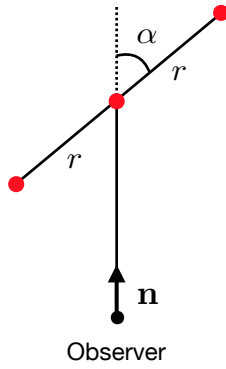


FIG. 1: Representation of the coordinate system used to express the line correlation function: $r = |\mathbf{r}|$ denotes the separation between galaxies, and $\cos \alpha = \hat{\mathbf{r}} \cdot \mathbf{n}$ is the orientation of the line with respect to the direction of observation \mathbf{n} . We work in the distant-observer approximation, in which \mathbf{n} is the same for all galaxies.

Since redshift-space distortions break isotropy, the line correlation function depends not only on the modulus of the separation $r = |\mathbf{r}|$, but also on the orientation of the vector \mathbf{r} with respect to the line-of-sight: $\cos \alpha = \hat{\mathbf{r}} \cdot \mathbf{n}$, as depicted in Fig. 1. In the rest of this paper, we will study the dependence of the line correlation function on α . Note that in the case where $f = 0$, Eq. (23) is equivalent to the expression derived in [18].

III. MULTIPOLE EXPANSION OF THE LINE CORRELATION FUNCTION

In redshift-space, the two-point correlation function of Δ can be written as the sum of a monopole, quadrupole and hexadecapole in the angle α . At linear order in perturbation theory and using the distant-observer approximation, one can show that these three multipoles encode all the information present in the two-point correlation function [7].

Contrary to the two-point correlation function, the line correlation function cannot be simply expressed as a sum of the first three even Legendre polynomials only. However, we will see that the contribution from the multipoles larger than $n = 4$ is actually negligible so that most of the information about redshift-space distortions is indeed encoded in the monopole, quadrupole and hexadecapole of ℓ .

Since the Legendre polynomials form a basis, we can expand the line correlation function as

$$\ell(r, \alpha, z) = \sum_{n=0}^{\infty} Q_n(r, z) L_n(\cos \alpha), \quad (24)$$

where $\cos \alpha = \hat{\mathbf{r}} \cdot \mathbf{n}$ and L_n denotes the Legendre polynomial of order n . The multipole of order n can be measured by weighting the line correlation function by the

appropriate Legendre polynomial

$$Q_n(r, z) = \frac{2n+1}{2} \int_{-1}^1 d\mu \ell(r, \mu, z) L_n(\mu), \quad (25)$$

where $\mu = \cos \alpha$.

To calculate explicitly Q_n , we insert Eq. (23) into (24) and we expand the exponentials in (23) and the Legendre polynomial in (24) in terms of spherical harmonics

$$e^{i\mathbf{k}\cdot\mathbf{r}} = 4\pi \sum_{n=0}^{\infty} \sum_{m=-n}^n i^n j_n(kr) Y_{nm}^*(\hat{\mathbf{k}}) Y_{nm}(\hat{\mathbf{r}}), \quad (26)$$

$$L_n(\mu) = \frac{4\pi}{2n+1} \sum_{m=-n}^n Y_{nm}(\mathbf{n}) Y_{nm}^*(\hat{\mathbf{r}}). \quad (27)$$

We obtain

$$Q_n(r, z) = \frac{r^{9/2}}{8\sqrt{2}(2\pi)^3} 8\pi^2 \sum_{m=-n}^n \sum_{n'=0}^{\infty} \sum_{m'=-n'}^n i^{n'} \int_{-1}^1 d\mu Y_{nm}^*(\hat{\mathbf{r}}) Y_{n'm'}(\hat{\mathbf{r}}) Y_{nm}(\mathbf{n}) \int \int_{\substack{|\mathbf{k}_1|, |\mathbf{k}_2| \\ |\mathbf{k}_1 + \mathbf{k}_2| \leq 2\pi/r}} d^3\mathbf{k}_1 d^3\mathbf{k}_2 W_2(-\mathbf{k}_1 - \mathbf{k}_2, \mathbf{k}_1, \mathbf{k}_2, \mathbf{n}) \sqrt{\frac{P_L(|\mathbf{k}_1 + \mathbf{k}_2|, z) P_L(k_1, z)}{P_L(k_2, z)}} \times \left[j_{n'}(\kappa_1 r) Y_{n'm'}^*(\hat{\boldsymbol{\kappa}}_1) + j_{n'}(\kappa_2 r) Y_{n'm'}^*(\hat{\boldsymbol{\kappa}}_2) + j_{n'}(\kappa_3 r) Y_{n'm'}^*(\hat{\boldsymbol{\kappa}}_3) \right], \quad (28)$$

where

$$\boldsymbol{\kappa}_1 \equiv \mathbf{k}_1 - \mathbf{k}_2, \quad (29)$$

$$\boldsymbol{\kappa}_2 \equiv \mathbf{k}_1 + 2\mathbf{k}_2, \quad (30)$$

$$\boldsymbol{\kappa}_3 \equiv -2\mathbf{k}_1 - \mathbf{k}_2. \quad (31)$$

Since in the distant-observer approximation, the direction of observation \mathbf{n} is fixed for all galaxies, we can choose \mathbf{n} on the $\hat{\mathbf{z}}$ axis without loss of generality. The integral over μ in Eq. (28) becomes then an integral over the direction of \mathbf{r} , which can be performed and gives rise to $\delta_{nn'} \delta_{mm'}$. Combining the remaining spherical harmonics into Legendre polynomials we obtain

$$Q_n(r, z) = \frac{r^{9/2} (2n+1)}{8\sqrt{2} (2\pi)^3} i^n \int \int_{\substack{|\mathbf{k}_1|, |\mathbf{k}_2| \\ |\mathbf{k}_1 + \mathbf{k}_2| \leq 2\pi/r}} d^3\mathbf{k}_1 d^3\mathbf{k}_2 W_2(-\mathbf{k}_1 - \mathbf{k}_2, \mathbf{k}_1, \mathbf{k}_2, \mathbf{n}) \sqrt{\frac{P_L(|\mathbf{k}_1 + \mathbf{k}_2|, z) P_L(k_1, z)}{P_L(k_2, z)}} \times \left[j_n(\kappa_1 r) L_n(\hat{\boldsymbol{\kappa}}_1 \cdot \mathbf{n}) + j_n(\kappa_2 r) L_n(\hat{\boldsymbol{\kappa}}_2 \cdot \mathbf{n}) + j_n(\kappa_3 r) L_n(\hat{\boldsymbol{\kappa}}_3 \cdot \mathbf{n}) \right]. \quad (32)$$

Equation (32) contains a 6-dimensional integral. We now show how to reduce it to a 3-dimensional integral that we can compute numerically.

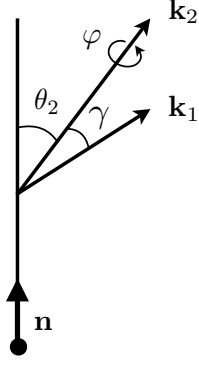


FIG. 2: Definition of the angles θ_2, γ and φ used in the calculation of the multipoles Q_n .

Let us denote by (θ_1, ϕ_1) and (θ_2, ϕ_2) the angular coordinates of \mathbf{k}_1 and \mathbf{k}_2 . Since we have fixed the direction of observation \mathbf{n} on the \hat{z} axis, we have $\hat{\mathbf{k}}_1 \cdot \mathbf{n} = \cos \theta_1$. We first do a change of variables from $\{\theta_1, \phi_1, \theta_2, \phi_2\} \rightarrow \{\gamma, \varphi, \theta_2, \phi_2\}$, where $\cos \gamma = \hat{\mathbf{k}}_1 \cdot \hat{\mathbf{k}}_2$ and φ is the azimuthal angle of \mathbf{k}_1 around \mathbf{k}_2 , see Fig. 2. The Jacobian of this transformation is 1, since it is a rotation. In Eq. (32), the only quantities that depend on φ and ϕ_2 are the Legendre polynomials. We have

$$\begin{aligned}\hat{\mathbf{k}}_1 \cdot \mathbf{n} &= \frac{-k_1 \sin \gamma \sin \theta_2 \cos(\varphi - \phi_2) + (k_1 \cos \gamma - k_2) \cos \theta_2}{\sqrt{k_1^2 + k_2^2 - 2k_1 k_2 \cos \gamma}}, \\ \hat{\mathbf{k}}_2 \cdot \mathbf{n} &= \frac{-k_1 \sin \gamma \sin \theta_2 \cos(\varphi - \phi_2) + (k_1 \cos \gamma + 2k_2) \cos \theta_2}{\sqrt{k_1^2 + 4k_2^2 + 4k_1 k_2 \cos \gamma}}, \\ \hat{\mathbf{k}}_3 \cdot \mathbf{n} &= \frac{2k_1 \sin \gamma \sin \theta_2 \cos(\varphi - \phi_2) - (2k_1 \cos \gamma + k_2) \cos \theta_2}{\sqrt{4k_1^2 + k_2^2 + 4k_1 k_2 \cos \gamma}}.\end{aligned}$$

For any value of n the integral over ϕ_2 and φ can be done analytically, since the Legendre polynomials can always be expressed as a series of cosines. For odd n 's we find that the integrals vanish, as expected due to the symmetry of the line correlation function. We present here the derivation and explicit expression for the monopole $n = 0$, the quadrupole $n = 2$ and the hexadecapole $n = 4$. In Appendix A we derive a general expression valid for any n .

A. The monopole of the line correlation function

For the monopole, the integral over ϕ_2 and φ in Eq. (32) trivially gives $4\pi^2$ since the Legendre polynomials are constant. The integral over θ_2 can then be performed analytically

$$\int_{-1}^1 d\mu_2 \frac{bF_2 + \mu_2^2 f G_2}{b + \mu_2^2 f} = 2 \left[G_2 + (F_2 - G_2) \frac{\arctan \sqrt{\beta}}{\sqrt{\beta}} \right]$$

where $\mu_2 = \cos \theta_2$ and

$$\beta \equiv \frac{f}{b}. \quad (33)$$

The monopole then simply becomes

$$\begin{aligned}Q_0(r, z) &= \frac{r^{9/2}}{8\pi\sqrt{2}} \int_0^{2\pi/r} dk_1 k_1^2 \int_0^{2\pi/r} dk_2 k_2^2 \int_{-1}^{\nu_{\text{cut}}} d\nu \\ &\sqrt{\frac{P_L(|\mathbf{k}_1 + \mathbf{k}_2|, z) P_L(k_1, z)}{P_L(k_2, z)}} \left\{ F_2(-\mathbf{k}_1 - \mathbf{k}_2, \mathbf{k}_1) \right. \\ &\left. + \left(\frac{\arctan \sqrt{\beta}}{\sqrt{\beta}} - 1 \right) (F_2 - G_2)(-\mathbf{k}_1 - \mathbf{k}_2, \mathbf{k}_1) \right\} \\ &\times \sum_{i=1}^3 j_0(\kappa_i r),\end{aligned} \quad (34)$$

where

$$\nu_{\text{cut}} = \min \left\{ 1, \max \left\{ -1, \left[(2\pi/r)^2 - k_1^2 - k_2^2 \right] / [2k_1 k_2] \right\} \right\}$$

enforces the condition $|\mathbf{k}_1 + \mathbf{k}_2| \leq 2\pi/r$. Here the kernel F_2 and G_2 , and the κ_i defined in Eqs. (29) to (31) can be expressed as functions of k_1, k_2 and $\nu = \cos \gamma = \hat{\mathbf{k}}_1 \cdot \hat{\mathbf{k}}_2$ only. Equation (34) contains three integrals that can be computed numerically.

B. The quadrupole of the line correlation function

To calculate the quadrupole, we first need to integrate the terms in the square bracket in Eq. (32) over ϕ_2 and φ . As an example, let us look at the first term. We have

$$\begin{aligned}\int_0^{2\pi} d\phi_2 \int_0^{2\pi} d\varphi L_2(\hat{\mathbf{k}}_1 \cdot \mathbf{n}) &= (2\pi)^2 \left[1 - \frac{3k_1^2(1-\nu^2)}{2\kappa_1^2} \right] \\ &\times L_2(\cos \theta_2).\end{aligned} \quad (35)$$

As for the monopole, the integral over θ_2 can then be performed analytically

$$\begin{aligned}\int_{-1}^1 d\mu_2 \frac{bF_2 + \mu_2^2 f G_2}{b + \mu_2^2 f} L_2(\mu_2) &= -\beta^{-3/2} \left[-3\sqrt{\beta} \right. \\ &\left. + (\beta + 3) \arctan \sqrt{\beta} \right].\end{aligned}$$

Similar expressions can be found for the second and third terms in the square bracket of (32). Putting everything together, we then obtain for the quadrupole

$$\begin{aligned}Q_2(r, z) &= \frac{r^{9/2}}{8\pi\sqrt{2}} \int_0^{2\pi/r} dk_1 k_1^2 \int_0^{2\pi/r} dk_2 k_2^2 \int_{-1}^{\nu_{\text{cut}}} d\nu \\ &\sqrt{\frac{P_L(|\mathbf{k}_1 + \mathbf{k}_2|, z) P_L(k_1, z)}{P_L(k_2, z)}} (F_2 - G_2)(-\mathbf{k}_1 - \mathbf{k}_2, \mathbf{k}_1) \\ &\frac{5}{2\beta^{3/2}} \left(-3\sqrt{\beta} + (\beta + 3) \arctan \sqrt{\beta} \right) \\ &\times \sum_{i=1}^3 j_2(\kappa_i r) \left(1 - \frac{3\rho_i^2}{2\kappa_i^2} \right),\end{aligned} \quad (36)$$

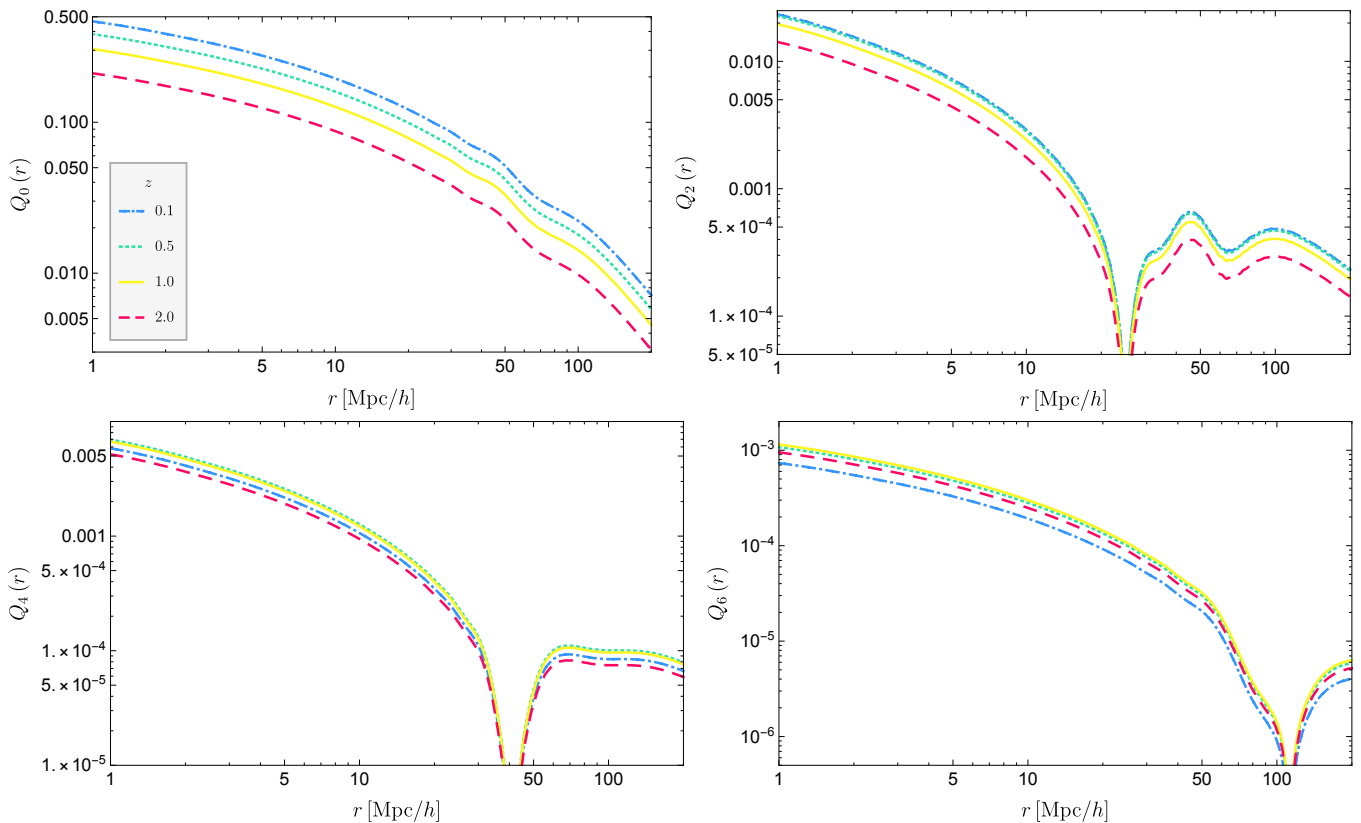


FIG. 3: Multipoles of the line correlation function, plotted as a function of separation r , for redshift $z = 0.1$ to $z = 2$. The monopole is positive at all separations. The quadrupole, hexadecapole and tetrahexadecapole are positive at small separations and negative at large separations.

where

$$\rho_1^2 = \rho_2^2 = k_1^2(1 - \nu^2) \quad \text{and} \quad \rho_3^2 = 4\rho_1^2. \quad (37)$$

Equation (36) contains again three integrals that can be computed numerically.

C. The hexadecapole of the line correlation function

The hexadecapole can be calculated in a very similar way as the quadrupole. The only difference is that the integral over ϕ_2 and φ in Eq. (35) contains Legendre polynomial of degree four instead of two. The resulting integral over μ_2 can again be done analytically and we

find

$$Q_4(r, z) = \frac{r^{9/2}}{8\pi\sqrt{2}} \int_0^{2\pi/r} dk_1 k_1^2 \int_0^{2\pi/r} dk_2 k_2^2 \int_{-1}^{\nu_{\text{cut}}} d\nu \sqrt{\frac{P_L(|\mathbf{k}_1 + \mathbf{k}_2|, z) P_L(k_1, z)}{P_L(k_2, z)}} (F_2 - G_2)(-\mathbf{k}_1 - \mathbf{k}_2, \mathbf{k}_1) \frac{9}{8\beta^{5/2}} \left[(3\beta^2 + 30\beta + 35) \arctan \sqrt{\beta} - \left(\frac{55}{3}\beta + 35 \right) \sqrt{\beta} \right] \times \sum_{i=1}^3 j_4(\kappa_i r) \left(1 - 5 \frac{\rho_i^2}{\kappa_i^2} + \frac{35}{8} \frac{\rho_i^4}{\kappa_i^4} \right). \quad (38)$$

D. General expression for the multipole Q_n

Following the same steps as for the monopole, quadrupole and hexadecapole, one can derive a general expression for the multipole of order n . The detail of the derivation is presented in Appendix A. Here we only give

the final expression

$$Q_{2n}(r, z) = \frac{r^{9/2}}{8\pi\sqrt{2}} \int_0^{2\pi/r} dk_1 k_1^2 \int_0^{2\pi/r} dk_2 k_2^2 \int_{-1}^{\nu_{\text{cut}}} d\nu \sqrt{\frac{P_L(|\mathbf{k}_1 + \mathbf{k}_2|, z) P_L(k_1, z)}{P_L(k_2, z)}} \frac{4n+1}{2} i^{2n} \mathcal{L}_{2n}(I) \sum_{i=1}^3 j_{2n}(\kappa_i r) \psi_{2n}\left(\frac{\rho_i}{\kappa_i}\right). \quad (39)$$

Here

$$\mathcal{L}_{2n}(I) = 2^{2n} \sum_{m=0}^n \binom{2n}{2m} \binom{n+m-\frac{1}{2}}{2n} I_{2m}, \quad (40)$$

with

$$I_{2m} = \frac{2}{2m+1} \left\{ G_2(-\mathbf{k}_1 - \mathbf{k}_2, \mathbf{k}_1) + \left[F_2(-\mathbf{k}_1 - \mathbf{k}_2, \mathbf{k}_1) - G_2(-\mathbf{k}_1 - \mathbf{k}_2, \mathbf{k}_1) \right] \times {}_2F_1\left(1, \frac{1}{2} + m, \frac{3}{2} + m; -\beta\right) \right\}, \quad (41)$$

where ${}_2F_1$ denotes the Gauss hypergeometric function and

$$\psi_{2n}\left(\frac{\rho_i}{\kappa_i}\right) = {}_2F_1\left(-n, n + \frac{1}{2}, 1; \left(\frac{\rho_i}{\kappa_i}\right)^2\right), \quad (42)$$

with the ρ_i defined in Eq. (37).

IV. RESULTS

We now calculate explicitly the multipoles of the line correlation function in a Λ CDM universe with parameters [47]: $\Omega_m = 0.3089$, $\Omega_b h^2 = 0.0223$, $h = 0.6774$, $n_s = 0.9667$, $\sigma_8 = 0.8159$ and $b = 1$. In Fig. 3 we show the monopole, quadrupole, hexadecapole and tetrahexadecapole ($n = 6$) at different redshifts. The monopole and quadrupole decrease with redshift, whereas the hexadecapole and tetrahexadecapole have a more complicated behaviour. The redshift dependence is governed by the coupling kernels F_2 and G_2 , the linear power spectrum, and the growth rate f , which enters in a different way in the different multipoles.

We see that the monopole dominates over the other multipoles by at least one order of magnitude. Note that the quadrupole, hexadecapole and tetrahexadecapole become negative at large separation, whereas the monopole is always positive. The r -dependence of the multipole n is governed by the sum of the spherical Bessel functions $j_n(\kappa_i r)$, weighted by different k and ν -dependent prefactors. It is therefore not surprising that the multipoles can

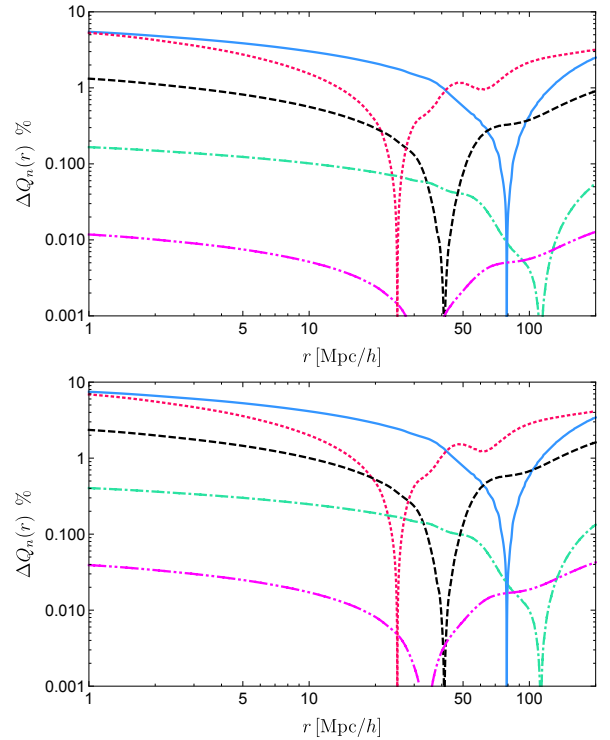


FIG. 4: Relative contribution due to redshift-space distortions (43), plotted as a function of separation r , at $z = 0.1$ (top panel) and $z = 1$ (bottom panel). The blue solid line shows the monopole contribution, the red dotted line the quadrupole contribution, the black dashed line the hexadecapole contribution, the green dot-dashed line the tetrahexadecapole contribution and the magenta double dot-dashed line the contribution for $n = 8$. The contributions are positive at small separations and negative at large separations.

change sign. Note that this is not specific to the line correlation function: the monopole of the two-point correlation function in redshift-space does indeed also change sign at large separation, see e.g. [48].

In Fig. 4 we show the relative contribution due to redshift-space distortions

$$\Delta Q_n = \frac{Q_n - Q_n^{\text{no rsd}}}{Q_0^{\text{no rsd}}}, \quad (43)$$

for $n = 0, 2, 4, 6$ and 8 . Note that $Q_0^{\text{no rsd}}$ is equivalent to Eq. (30) for $\ell(r, z)$ in [18]. We see that redshift-space distortions generate a correction of 7 percent in the monopole, at small separation and high redshift. The quadrupole and hexadecapole are a few percent of the monopole. The tetrahexadecapole is always less than a percent of the monopole, and the multipole $n = 8$ is less than 0.1 percent. Most of the information about redshift-space distortions is therefore captured by the first three even multipoles.

In Fig. 5 we show the relative contributions ΔQ_n at different redshifts. We see that in all cases the contributions due to redshift-space distortions increase as the redshift increases.

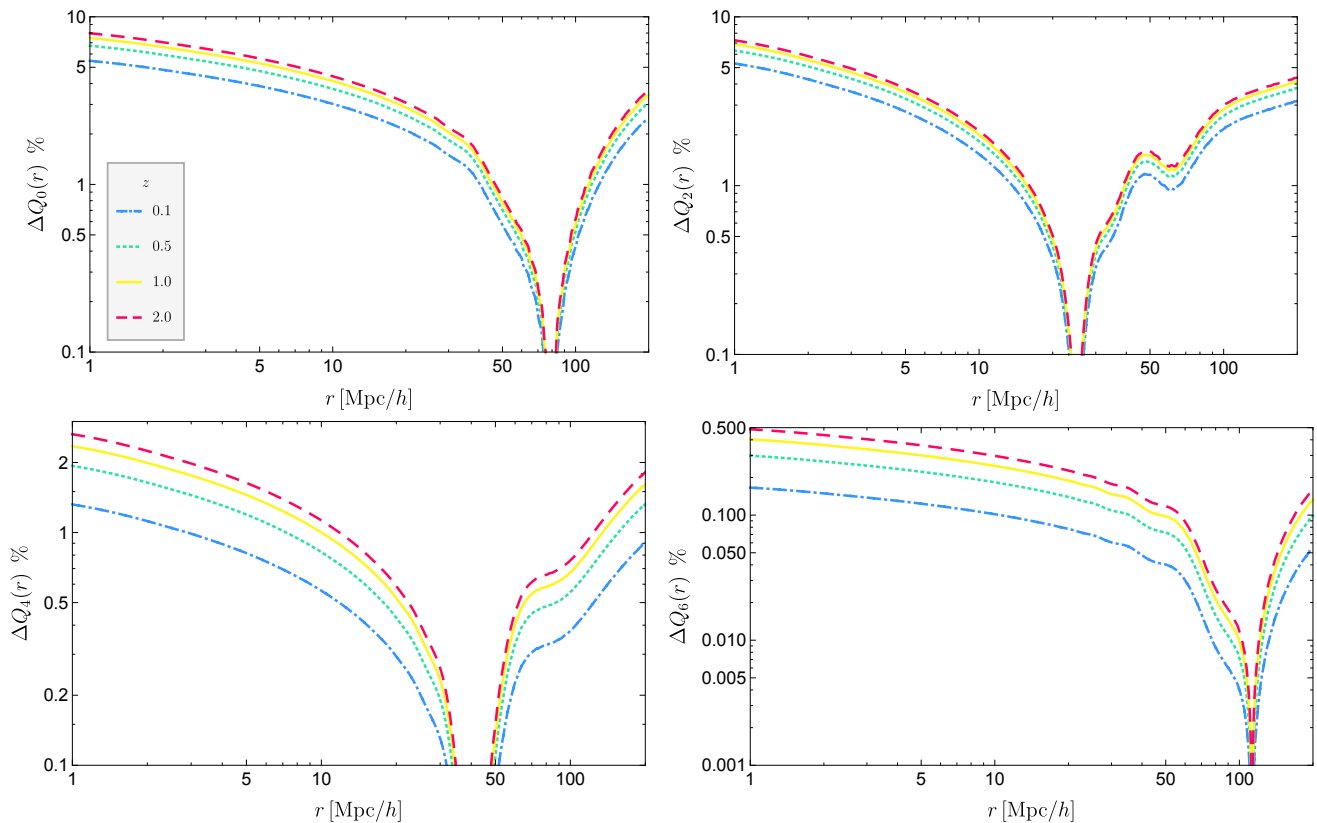


FIG. 5: The relative contribution due to redshift-space distortions, plotted as a function of separation r , for redshift $z = 0.1$ to $z = 2$. The contributions are positive at small separations and negative at large separations.

The reason for which the contribution due to redshift-space distortions is suppressed with respect to the density contribution can be understood by looking at the expression for the multipoles, Eqs. (34), (36) and (38). These expressions are all proportional to the *difference* between the density kernel F_2 and the velocity kernel G_2 . This follows from the fact that the correlation between phases in Eq. (13) is proportional to the weighted bispectrum $b_\Delta \propto B_\Delta / \sqrt{P_\Delta P_\Delta P_\Delta}$. This weighted bispectrum probes the difference between the linear relation between V and δ and the non-linear relation. If these relations are the same, then $F_2 = G_2$ and the function W_2 defined in Eq. (22) reduces simply to F_2 . We recover then the expression for the line correlation function in real-space. Hence by measuring the line correlation function in redshift-space we probe the fact that the relation between the density δ and the peculiar velocity V is different at linear and at second order in perturbation theory. In other words, we probe the difference between the continuity and Euler equation at linear and second-order in perturbation theory.

As such the line correlation function is complementary to the two-point correlation function in redshift-space. The two-point correlation function probes indeed the linear relation between density and velocity by measuring the growth rate f . The line correlation function adds

information since it probes the non-linear relation between the density and velocity by measuring the difference $F_2 - G_2$. This clearly shows that phase correlations encode a different type of information than the two-point correlation function. Modified theories of gravity generically modify both the growth rate f [49–51] and the coupling kernels F_2 and G_2 [46]. Hence the line correlation function in redshift-space is expected to be useful to constrain modifications of gravity.

In Fig. 6, we compare the contribution to the monopole (34) generated by the kernel F_2 only, by the kernel G_2 and by the difference $F_2 - G_2$. We see that the difference is significantly smaller than the individual contributions from F_2 and G_2 . This explains the suppression of the redshift-space distortion signal, with respect to the signal in real-space. Note that here we are using second-order perturbation theory, which does not account for the effect of Fingers of God at small scales. As shown in [11, 12], those have a strong impact on the bispectrum in the non-linear regime. In a future work, we will study the line correlation function beyond perturbation theory, accounting for the Fingers of God, to see if they enhance the multipoles.

In Fig. 7, we plot the prefactors for the monopole, quadrupole and hexadecapole, which depend on the

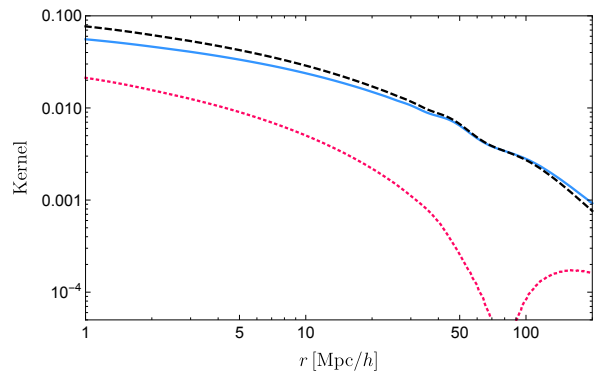


FIG. 6: Monopole of the line correlation function (34), at redshift $z = 1$, generated by the kernel F_2 (blue solid line), G_2 (black dashed line) and the difference $F_2 - G_2$ (red dotted line). The contributions from F_2 and G_2 are negative, while the difference is positive at small separations and negative at large separations.

growth rate $\beta = f/b$

$$A_0 = \frac{\arctan \sqrt{\beta}}{\sqrt{\beta}} - 1, \quad (44)$$

$$A_2 = \frac{5}{2\beta^{3/2}} \left[-3\sqrt{\beta} + (\beta + 3) \arctan \sqrt{\beta} \right], \quad (45)$$

$$A_4 = \frac{9}{8\beta^{5/2}} \left[-\left(\frac{55f}{3} + 35 \right) \sqrt{f} + (3f^2 + 30f + 35) \arctan \sqrt{\beta} \right]. \quad (46)$$

We see that these prefactors evolve slowly with redshift, showing that the line correlation function is less sensitive than the two-point correlation function to variations in the growth rate. We also see that these prefactors are smaller than 1 at all redshift, which also explains why the redshift-space correction is significantly smaller than the density contribution.

Note that the different dependence of the multipoles in the growth rate is very interesting, since it provides a way of disentangling it from the parameter σ_8 . The two-point correlation function measures indeed the combination $f\sigma_8$ (see e.g. [8]). The monopole of the bispectrum has been shown to measure a different combination, $f^{0.43}\sigma_8$, which in combination with the two-point function allows to disentangle f and σ_8 [52]. Here we see, from Eqs. (34), (36) and (38), that the multipoles of the line correlation function are sensitive to yet three other combinations of f and σ_8 . Combining these measurements has therefore the potential to tighten the individual constraints on f and σ_8 . In a future work, we will do a detail forecast on the constraints we expect from the line correlation function on f , σ_8 and the coupling kernels F_2 and G_2 .

Finally, in Fig. 8 we show the relative contribution from redshift-space distortion as a function of the orien-

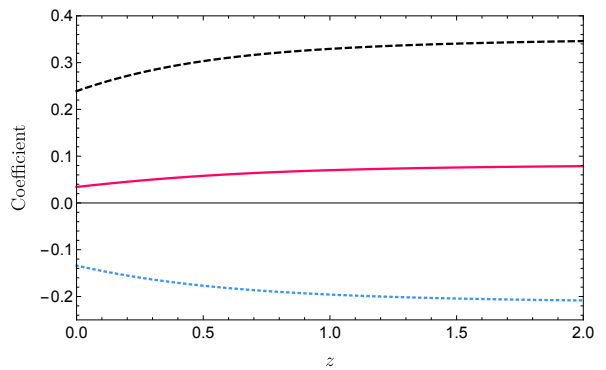


FIG. 7: Coefficients proportional to the growth rate $\beta = f/b$, in front of the monopole (44) (blue dotted line), quadrupole (45) (black dashed line) and hexadecapole (46) (red solid line), plotted as a function of redshift.

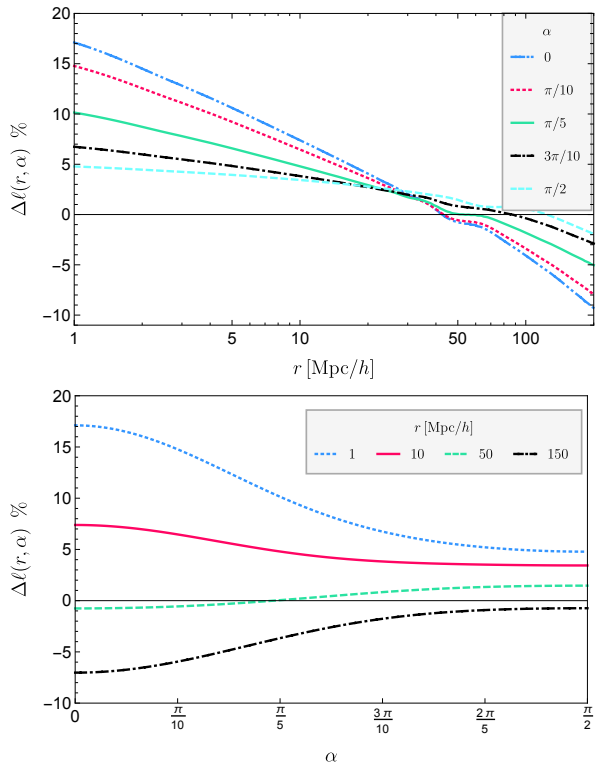


FIG. 8: Relative contribution from redshift-space distortion (47), plotted as a function of separation r for fixed values of the orientation α (upper panel); and as a function of the orientation α for fixed separation r (lower panel). The plots are at redshift $z = 1$.

tation² of the line α and the separation r

$$\Delta\ell(r, \alpha, z) = \frac{\ell(r, \alpha, z) - \ell^{\text{no rsd}}(r, z)}{\ell^{\text{no rsd}}(r, z)}. \quad (47)$$

We see that redshift-space distortions has the largest impact at small separation and when the three-points are aligned with respect to the direction of observation ($\alpha = 0$). In this case, the contribution from redshift-space distortions can reach 17 percent. This reflects the fact that redshift-space distortions modify the apparent radial distance between galaxies, but not their apparent angular separation. As a consequence, it is the largest when the galaxies are at different radial distances but in the same direction.

One would then naively expect that in the other extreme, i.e. when $\alpha = \pi/2$, the redshift-space contribution $\Delta\ell(r, \alpha, z)$ would vanish. This corresponds indeed to the case where the three points are at the same redshift, but in different directions. From the cyan dashed line in the top panel of Fig. 8 we see however that $\Delta\ell(r, \pi/2, z) \neq 0$. This can be understood in the following way: suppose that the three pixels, which are at the same redshift, are all situated in an over-dense region. As a consequence the galaxies inside each pixel are falling toward the center of the pixel. The pixels in redshift-space look therefore denser than they are in real space. Now since the three pixels are situated in the same over-dense region, this effect induces a correlation between the three pixels. This in turns generates an additional correlation between the phases of Δ . This effect is independent of the orientation of \mathbf{r} with respect to \mathbf{n} . It simply comes from the fact that correlated density fields generate correlated velocity fields. Hence, even though at $\alpha = \pi/2$ there is no change in the apparent distance between the pixels, there is still an effect due to the fact that the size of each pixel changes in a correlated way. Note that this effect is not specific to the line correlation function, but it also exists in the two-point correlation function of galaxies: the redshift-space two-point correlation function at $\alpha = \pi/2$ is not the same as the real-space two-point correlation function $\xi(r, \alpha = \pi/2) \neq \xi^{\text{no rsd}}(r)$.

V. CONCLUSIONS

In this paper, we have derived an expression for the line correlation function in redshift-space, which is valid at second-order in perturbation theory. We have expanded the line correlation function in Legendre polynomials and we have derived a generic expression for the multipoles Q_n . We have calculated explicitly the first multipoles in a Λ CDM universe and we have found that

the monopole, quadrupole and hexadecapole encode almost all of the information in redshift-space.

We have shown that the multipoles are sensitive to the difference $F_2 - G_2$, i.e. to the difference between the non-linear evolution of the density field and the non-linear evolution of the velocity field. As such the line correlation function is highly complementary to the two-point correlation function, which is sensitive to the linear growth rate of the density and velocity fields. This shows that correlations between phases encode different information than the two-point correlation function. Our expressions for the multipoles further show that each of them is sensitive to a different combination of the growth rate f and of σ_8 . Combining this with a measurement of the two-point correlation function, which is sensitive to the product $f\sigma_8$ can therefore break the degeneracy between these two parameters. In a future work, we will forecast how well this can be achieved with current and future surveys.

Our derivation relies on second-order perturbation theory. It is however well known that redshift-space distortions are not fully described by the second-order coupling kernel G_2 even on mildly non-linear scales [10–12]. In a future work, we will investigate how the multipoles change if we introduce non-linear effects, like Fingers of God. We expect such effects to enhance the redshift-space distortion signal, since they will increase the difference $F_2 - G_2$.

Finally, let us note that the line correlation function targets a very particular choice of phase correlations, namely those that appear along a line, i.e. along filaments. It may be interesting to investigate other configurations, where the redshift-space distortions signal may be enhanced with respect to the real-space signal.

Acknowledgements

We thank Joyce Byun and Pierre Fleury for useful discussions. CB and FOF acknowledge support by the Swiss National Science Foundation. DO thanks for support the Research Collaboration Award PG12105206 of the University of Western Australia.

Appendix A: Calculation of the multipoles Q_n

In Section III we have performed a multipole expansion for the line correlation function. All information of our statistical measure $\ell(\mathbf{r}, z)$ can be encoded in a (infinite) sum of multipoles $Q_n(r, z)$ given by (32). Here we show how three of the six integrals in this expression can be solved analytically for any order of multipole Q_n , namely the angular integrals θ_2 , ϕ_2 and φ .

Since only the kernel W_2 and the Legendre polynomial L_n are functions of these angles, the challenge is to solve

² Since the multipoles larger than $n = 6$ are negligible, we can write the line correlation function as $\ell(r, \alpha, z) = Q_0(r, z) + Q_2(r, z)L_2(\cos \alpha) + Q_4(r, z)L_4(\cos \alpha) + Q_6(r, z)L_6(\cos \alpha)$.

the following expression

$$M_n^{\kappa_i} = \int_0^\pi \sin \theta_2 d\theta_2 W_2(-\mathbf{k}_1 - \mathbf{k}_2, \mathbf{k}_1, \mathbf{k}_2, \mathbf{n}) \int_0^{2\pi} d\phi_2 \int_0^{2\pi} d\varphi L_n(\hat{\boldsymbol{\kappa}}_i \cdot \mathbf{n}). \quad (\text{A1})$$

The kernel W_2 is provided by (22) and the vectors $\boldsymbol{\kappa}_i$ are defined in (29)-(31). The angles $\hat{\boldsymbol{\kappa}}_i \cdot \mathbf{n}$ can be written as

$$\hat{\boldsymbol{\kappa}}_i \cdot \mathbf{n} \equiv \cos \theta_{\kappa_i} = \frac{\rho_i \sin \theta_2 \cos(\varphi - \phi_2) + \varrho_i \cos \theta_2}{\kappa_i}, \quad (\text{A2})$$

where

$$\begin{aligned} \rho_1 &= -k_1 \sin \gamma, & \varrho_1 &= k_1 \cos \gamma - k_2, \\ \rho_2 &= -k_1 \sin \gamma, & \varrho_2 &= k_1 \cos \gamma + 2k_2, \\ \rho_3 &= 2k_1 \sin \gamma, & \varrho_3 &= -2k_1 \cos \gamma - k_2, \end{aligned} \quad (\text{A3})$$

with constraint $\kappa_i^2 = \rho_i^2 + \varrho_i^2$.

In order to solve the integrals, we express the Legendre polynomials as

$$L_n(\hat{\boldsymbol{\kappa}}_i \cdot \mathbf{n}) = 2^n \sum_{m=0}^n \binom{n}{m} \binom{\frac{n+m-1}{2}}{n} \cos^m \theta_{\kappa_i}. \quad (\text{A4})$$

Due to the binomial coefficients, the only terms that contribute to the sum will be those with the same parity as n . Using the binomial expansion, $\cos^a \theta_{\kappa_i}$ can be rewritten as

$$\begin{aligned} \cos^m \theta_{\kappa_i} &= \kappa_i^{-m} \sum_{u=0}^m \binom{m}{u} (\varrho_i \cos \theta_2)^{m-u} (\rho_i \sin \theta_2)^u \\ &\quad \times \cos^u(\varphi - \phi_2). \end{aligned} \quad (\text{A5})$$

Therefore, the integrals over the axial angles ϕ_2 and φ can be trivially solved and it yields

$$\begin{aligned} \int_0^{2\pi} d\phi_2 \int_0^{2\pi} d\varphi \cos^b(\varphi - \phi_2) &= \frac{1 + (-1)^u}{2} \\ &\quad (2\pi)^2 \binom{u-1}{-1/2} / 2. \end{aligned} \quad (\text{A6})$$

The integral over θ_2 takes the form³

$$\int_0^\pi d\theta_2 \sin \theta_2 \frac{b F_2 + \cos^2(\theta_2) f G_2}{b + \cos^2(\theta_2) f} \cos^{m-u}(\theta_2) \sin^u(\theta_2). \quad (\text{A7})$$

These two expressions above reveal an important feature about the parity of LCF. First, Eq. (A6) tells us that only even values of u contribute to the sum (A5). Second, due to the orthogonality of the trigonometric functions, Eq. (A7) will not vanish if and only if $m - u$ is

even, which implies that m must also be even. Thus we conclude that in the multipole expansion (32), only even multipoles contribute to the sum. This reflects the fact that the line correlation function is symmetric under the exchange of the three galaxies on the line.

Thereby, without loss of generality, one can consider a relabelling: $n \rightarrow 2n$, $m \rightarrow 2m$ and $u \rightarrow 2u$. We can then use that $\varrho_i^{2(m-u)} = (\kappa_i^2 - \rho_i^2)^{m-u}$, so that

$$\kappa_i^{-2m} \varrho_i^{2(m-u)} \rho_i^{2u} = \sum_{w=0}^{m-u} \binom{m-u}{w} (-1)^w \left(\frac{\rho_i}{\kappa_i} \right)^{2(u+w)}. \quad (\text{A8})$$

In the interval $\theta_2 \in [0, \pi]$ the sine function can be written as $\sin \theta_2 = \sqrt{1 - \cos^2(\theta_2)}$ and consequently

$$\sin^{2u}(\theta_2) = \sum_{v=0}^u \binom{u}{v} (-1)^v \cos^{2v}(\theta_2). \quad (\text{A9})$$

We are now able to solve the integral over θ_2 which is of the form

$$\begin{aligned} \int_{-1}^1 d\mu_2 \frac{b F_2 + \mu_2^2 f G_2}{b + \mu_2^2 f} \mu_2^{2j} &= \frac{2}{j+1} \\ &\quad \left[G_2 + (F_2 - G_2) {}_2\mathcal{F}_1 \left(1, \frac{1}{2} + j, \frac{3}{2} + j; -\beta \right) \right], \end{aligned} \quad (\text{A10})$$

where in our case $j = m + v - u$. Here ${}_2\mathcal{F}_1$ denotes the Gauss hypergeometric function defined by

$${}_2\mathcal{F}_1(a, b, c; z) = \sum_{n=0}^{\infty} \frac{(a)_n (b)_n}{(c)_n} \frac{z^n}{n!}, \quad (\text{A11})$$

where $(a)_n = \Gamma(a+n)/\Gamma(a)$ is the Pochhammer symbol.

Finally, collecting all these results, $M_{2n}^{\kappa_i}$ can be written as

$$\begin{aligned} M_{2n}^{\kappa_i} &= 2 (2\pi)^2 2^{2n} \sum_{m=0}^n \sum_{u=0}^m \sum_{w=0}^{m-u} \sum_{v=0}^u \binom{2n}{2m} \binom{n+m-\frac{1}{2}}{2n} \\ &\quad \binom{2m}{2u} \binom{u-\frac{1}{2}}{-\frac{1}{2}} \binom{m-u}{w} \binom{u}{v} (-1)^{w+v} \left(\frac{\rho_i}{\kappa_i} \right)^{2(u+w)} \\ &\quad \frac{1}{2(m+v-u)+1} \left\{ G_2(-\mathbf{k}_1 - \mathbf{k}_2, \mathbf{k}_1) \right. \\ &\quad \left. + \left[F_2(-\mathbf{k}_1 - \mathbf{k}_2, \mathbf{k}_1) - G_2(-\mathbf{k}_1 - \mathbf{k}_2, \mathbf{k}_1) \right] \right. \\ &\quad \left. \times {}_2\mathcal{F}_1 \left(1, \frac{1}{2} + m + v - u, \frac{3}{2} + m + v - u; -\beta \right) \right\}. \end{aligned} \quad (\text{A12})$$

This expression can be further simplified through a long algebraic manipulation and indices relabeling and we obtain

$$M_{2n}^{\kappa_i} = (2\pi)^2 \mathcal{L}_{2n}(I) \psi_{2n} \left(\frac{\rho_i}{\kappa_i} \right), \quad (\text{A13})$$

³ To simplify the notation we drop the argument in F_2 and G_2 which are both functions of $(-\mathbf{k}_1 - \mathbf{k}_2, \mathbf{k}_1)$.

where

$$\mathcal{L}_{2n}(I) = 2^{2n} \sum_{m=0}^n \binom{2n}{2m} \binom{n+m-\frac{1}{2}}{2n} I_{2m} \quad (\text{A14})$$

with

$$I_{2m} = \frac{2}{2m+1} \left\{ G_2(-\mathbf{k}_1 - \mathbf{k}_2, \mathbf{k}_1) + \left[F_2(-\mathbf{k}_1 - \mathbf{k}_2, \mathbf{k}_1) - G_2(-\mathbf{k}_1 - \mathbf{k}_2, \mathbf{k}_1) \right] \times {}_2\mathcal{F}_1 \left(1, \frac{1}{2} + m, \frac{3}{2} + m; -\beta \right) \right\}, \quad (\text{A15})$$

and

$$\psi_{2n} \left(\frac{\rho_i}{\kappa_i} \right) = {}_2\mathcal{F}_1 \left(-n, n + \frac{1}{2}, 1; \left(\frac{\rho_i}{\kappa_i} \right)^2 \right). \quad (\text{A16})$$

This shows that the multipoles can be calculated from expression (39).

-
- [1] D. H. Jones et al., *Mon. Not. Roy. Astron. Soc.* **399**, 683 (2009), 0903.5451.
- [2] K. N. Abazajian et al. (SDSS), *Astrophys. J. Suppl.* **182**, 543 (2009), 0812.0649.
- [3] D. Parkinson, S. Riemer-Sørensen, C. Blake, G. B. Poole, T. M. Davis, S. Brough, M. Colless, C. Contreras, W. Couch, S. Croom, et al., *Phys. Rev. D* **86**, 103518 (2012), 1210.2130.
- [4] M. Scodreggio, L. Guzzo, B. Garilli, B. R. Granett, M. Bolzonella, S. de la Torre, U. Abbas, C. Adami, S. Arnouts, D. Bottini, et al., *Astron. and Astrophys.* **609**, A84 (2018), 1611.07048.
- [5] S. Alam, F. D. Albareti, C. Allende Prieto, F. Anders, S. F. Anderson, T. Anderton, B. H. Andrews, E. Armengaud, É. Aubourg, S. Bailey, et al., *Astrophys. J.* **219**, 12 (2015), 1501.00963.
- [6] N. Kaiser, *Mon. Not. Roy. Astron. Soc.* **227**, 1 (1987).
- [7] A. J. S. Hamilton, in *Ringberg Workshop on Large Scale Structure Ringberg, Germany, September 23-28, 1996* (1997), astro-ph/9708102.
- [8] S. Alam et al. (BOSS), *Mon. Not. Roy. Astron. Soc.* **470**, 2617 (2017), 1607.03155.
- [9] A. G. Sanchez et al. (BOSS), *Mon. Not. Roy. Astron. Soc.* **464**, 1640 (2017), 1607.03147.
- [10] R. Scoccimarro, H. M. P. Couchman, and J. A. Frieman, *Astrophys. J.* **517**, 531 (1999), astro-ph/9808305.
- [11] E. Gaztanaga and R. Scoccimarro, *Mon. Not. Roy. Astron. Soc.* **361**, 824 (2005), astro-ph/0501637.
- [12] H. Gil-Marín, C. Wagner, J. Noreña, L. Verde, and W. Percival, *JCAP* **1412**, 029 (2014), 1407.1836.
- [13] C. Hikage, Y. Suto, I. Kayo, A. Taruya, T. Matsubara, M. S. Vogeley, F. Hoyle, J. R. Gott, III, and J. Brinkmann (SDSS), *Publ. Astron. Soc. Jap.* **54**, 707 (2002), astro-ph/0207377.
- [14] S. Codis, C. Pichon, D. Pogosyan, F. Bernardeau, and T. Matsubara, *Mon. Not. Roy. Astron. Soc.* **435**, 531 (2013), 1305.7402.
- [15] M. White, *JCAP* **1611**, 057 (2016), 1609.08632.
- [16] M. Scrimgeour et al., *Mon. Not. Roy. Astron. Soc.* **425**, 116 (2012), 1205.6812.
- [17] D. Obreschkow, C. Power, M. Bruderer, and C. Bonvin, *Astrophys. J.* **762**, 115 (2013), 1211.5213.
- [18] R. Wolstenhulme, C. Bonvin, and D. Obreschkow, *Astrophys. J.* **804**, 132 (2015), 1409.3007.
- [19] R. J. Scherrer, A. L. Melott, and S. F. Shandarin, *Astrophys. J.* **377**, 29 (1991).
- [20] B. S. Ryden and M. Gramann, *Astrophys. J.* **383**, L33 (1991).
- [21] J. Soda and Y. Suto, *Astrophys. J.* **396**, 379 (1992).
- [22] B. Jain and E. Bertschinger, *Astrophys. J.* **509**, 517 (1998), astro-ph/9808314.
- [23] L.-Y. Chiang and P. Coles, *MNRAS* **311**, 809 (2000), astro-ph/9905250.
- [24] P. Coles and L.-Y. Chiang, *Nature* **406**, 376 (2000), astro-ph/0006017.
- [25] L.-Y. Chiang, *MNRAS*. **325**, 405 (2001), astro-ph/0011021.
- [26] P. Watts, P. Coles, and A. Melott, *Astrophys. J.* **589**, L61 (2003), astro-ph/0211408.
- [27] L.-Y. Chiang, P. Naselsky, and P. Coles, *Astrophys. J.* **602**, L1 (2004), astro-ph/0208235.
- [28] L.-Y. Chiang, P. Coles, and P. Naselsky, *MNRAS* **337**, 488 (2002), astro-ph/0207584.
- [29] P. Coles, P. Dineen, J. Earl, and D. Wright, *MNRAS* **350**, 983 (2004), astro-ph/0310252.
- [30] T. Matsubara, *Astrophys. J.* **591**, L79 (2003), astro-ph/0303278.
- [31] C. Hikage, T. Matsubara, and Y. Suto, *Astrophys. J.* **600**, 553 (2004), astro-ph/0308472.
- [32] C. Hikage, T. Matsubara, Y. Suto, C. Park, A. S. Szalay, and J. Brinkmann, *Publ. Astron. Soc. Jap.* **57**, 709 (2005), astro-ph/0506194.
- [33] R. M. Szepletowski, D. J. Bacon, J. P. Dietrich, M. Busha, R. Wechsler, et al. (2013), 1306.5324.
- [34] A. Eggemeier and R. E. Smith, *Mon. Not. Roy. Astron. Soc.* **466**, 2496 (2017), 1611.01160.
- [35] J. Byun, A. Eggemeier, D. Regan, D. Seery, and R. E. Smith, *Mon. Not. Roy. Astron. Soc.* **471**, 1581 (2017), 1705.04392.
- [36] K. Ali, D. Obreschkow, C. Howlett, C. Bonvin, C. Llinares, F. Oliveira Franco, and C. Power, Submitted to *MNRAS* (????).
- [37] A. Eggemeier, T. Battefeld, R. E. Smith, and J. Niemeyer, *Mon. Not. Roy. Astron. Soc.* **453**, 797 (2015), 1504.04036.
- [38] J. Yoo, A. L. Fitzpatrick, and M. Zaldarriaga, *Phys. Rev.* **D80**, 083514 (2009), 0907.0707.
- [39] C. Bonvin and R. Durrer, *Phys. Rev.* **D84**, 063505

- (2011), 1105.5280.
- [40] A. Challinor and A. Lewis, *Phys. Rev.* **D84**, 043516 (2011), 1105.5292.
- [41] J. T. Nielsen and R. Durrer, *JCAP* **1703**, 010 (2017), 1606.02113.
- [42] R. J. Scherrer and E. Bertschinger, *Astrophys. J.* **381**, 349 (1991).
- [43] R. Juszkiewicz, D. H. Weinberg, P. Amsterdamski, M. Chodorowski, and F. Bouchet, *Astrophys. J.* **442**, 39 (1995), astro-ph/9308012.
- [44] F. Bernardeau and L. Kofman, *Astrophys. J.* **443**, 479 (1995), astro-ph/9403028.
- [45] F. Bernardeau, S. Colombi, E. Gaztanaga, and R. Scocimarro, *Phys. Rept.* **367**, 1 (2002), astro-ph/0112551.
- [46] F. Bernardeau and P. Brax, *JCAP* **1106**, 019 (2011), 1102.1907.
- [47] P. A. R. Ade et al. (Planck), *Astron. Astrophys.* **594**, A13 (2016), 1502.01589.
- [48] L. Samushia et al., *Mon. Not. Roy. Astron. Soc.* **439**, 3504 (2014), 1312.4899.
- [49] J. Gleyzes, D. Langlois, M. Mancarella, and F. Vernizzi, *JCAP* **1602**, 056 (2016), 1509.02191.
- [50] D. Alonso, E. Bellini, P. G. Ferreira, and M. Zumalacárregui, *Phys. Rev.* **D95**, 063502 (2017), 1610.09290.
- [51] J. S. Y. Leung and Z. Huang, *Int. J. Mod. Phys.* **D26**, 1750070 (2017), 1604.07330.
- [52] H. Gil-Marín, J. Norena, L. Verde, W. J. Percival, C. Wagner, M. Manera, and D. P. Schneider, *Mon. Not. Roy. Astron. Soc.* **451**, 539 (2015), 1407.5668.